



A new technique to measure in situ soil gas permeability



M. Castelluccio^a, G. De Simone^a, C. Lucchetti^a, M. Moroni^b, F. Salvati^a, P. Tuccimei^{a,*}

^a Università "Roma Tre", Dipartimento di Scienze, 00145 Roma, Italy

^b GEOEX s.a.s., C.so Matteotti 44, 00041 Albano Laziale, Roma, Italy

ARTICLE INFO

Article history:

Received 6 March 2014

Accepted 3 August 2014

Available online 10 August 2014

Keywords:

Soil permeability

Gas transport

Permeameter

Environmental pollution

ABSTRACT

Intrinsic permeability is crucial to assess gases and volatile compounds transport through soil. In situ measurements of this parameter are based on Darcy equation, an empirical relation that describes the flow of a fluid through a porous medium. A new technique for in situ measurement of soil gas permeability was developed and deeply tested in several terrains. The new instrument was successfully calibrated against RADON JOK, a permeameter which is widely employed all over the world. The new device provides rapid responses and is easy to carry in the field. It can be employed in the range of 3×10^{-13} – 8.0×10^{-11} m², extending the upper detection limit of RADON JOK (1.8×10^{-11}). Its use is recommended to investigate radon and other gas transfer through the soil and to map radon or CO₂ potentials of a given site. It could be also employed in environmental studies where the transfer of volatile pollutants is of primary concern.

© 2014 Elsevier B.V. All rights reserved.

Contents

1. Introduction	56
2. Theory	57
3. Field techniques.	57
4. Results and discussion.	58
References.	59

1. Introduction

Measurements of soil permeability to gases have taken on added significance in recent years as a result of increased efforts to determine entry rates of radon into buildings and to develop methods of mapping the radon potential of soils (Mosley et al., 1996).

Pollutants in groundwater can be a source of exposure to residents of houses overlying contaminated aquifers. Volatile compounds may migrate through soil gas and enter below-grade basements under negative pressure. Soil permeability was found to be the overriding factor controlling advective TCE intrusion into basements (Fischer and Uchirin, 1996).

Evaluation of gas movement is also important for estimating transport of volatile and semivolatile organic compounds from contaminated sites through the unsaturated zone to the groundwater. The use of soil venting, or soil vapor extraction, as a technique for

remediating contaminated sites has resulted in increased interest in gas transport in the unsaturated zone (Rathfelder et al., 1995). Migration of gases from landfills, such as methane formed by decomposition of organic material, is important in many areas (Moore et al., 1982; Thibodeaux et al., 1982). Soil gas composition has also been used as a tool for mapping organic contaminant plumes and for mineral and petroleum exploration.

In addition to that, pesticide volatilization contributes to air pollution, especially in areas of intensive agriculture. Of all the pesticides, soil fumigants are potentially the most volatile because of their high vapor pressures. Soil fumigation is used for controlling soilborne pathogens and parasitic nematodes, and the practice is essential for the production of high value crops such as strawberry and tomato, among many others (Gan et al., 1982).

Since the measurement of soil gas permeability is crucial in all these cases concerning environmental hazard and remediation, we developed and tested a new apparatus to determine the in situ intrinsic permeability of subsoil, which has the advantage to take into consideration the influence of natural moisture, density, and

* Corresponding author. Tel.: +39 6 5733 8092; fax: +39 6 5733 8201.
E-mail address: paola.tuccimei@uniroma3.it (P. Tuccimei).

effective porosity of soil, compared with indirect estimation such as particle size analysis.

2. Theory

Theoretical framework for gas permeability measurement is based on Darcy's equation. The soil is assumed to be homogeneous and isotropic and a standard state is considered. Furthermore the air is assumed to be incompressible (pressure differences are very much smaller than the atmospheric pressure). The gas permeability of soil, k (m^2), is calculated from the equation below (Damkjær and Korsbech, 1992; Neznal et al., 2004):

$$k = \frac{\mu \cdot Q}{F \cdot \Delta P} \quad (1)$$

where μ (Pa s) is the dynamic viscosity of air (at 10 °C, $\mu = 1.75 \times 10^{-5}$ Pa s), Q ($\text{m}^3 \text{s}^{-1}$) is the air flow through the probe, F (m) is the shape factor of the probe and ΔP (Pa) is the pressure difference between surface and the active area of the probe.

Critical point is the determination of the shape factor F . A solution was found in Damkjær and Korsbech (1992). Resultant formula is as follows:

$$F = \frac{2\pi L}{\ln \left(\frac{2L \sqrt{\frac{(4D-L)}{(4D+L)}}}{d} \right)} \quad (2)$$

where L (m) is the length of the active area of the probe head, D (m) is the depth below the surface and d (m) is the diameter of the active area. It is worth stressing that that active area is the internal surface area of the measuring cavity which is created at the lower end of the sampling probe to enable the air collection. Further details on air withdrawal from the soil are provided in the next section.

3. Field techniques

The principle of this equipment consists of air withdrawal by means of negative pressure. Air is pumped out from the soil through



Fig. 1. Setting up the experimental system for permeability measurement—Photo sequence. Inserting the sharp tip into the lower end of the sampling probe (a and b); the probe with the tip is prepared at the sampling place (c); preparing the drive in head (d); the probe is pounded to the desired depth using a hammer (e); inserting of the punch wire into the probe (f); inserting of the distance ring (g); fixing the distance screw till it touches the distance ring (h); the sharp tip is moved to the exact distance using the punch wire and the adjusted distance screw (i and j); when done, the sharp tip is extruded and, after removal of the punch wire, a cylindrical cavity of known volume, with defined length, L , and diameter, d , is created (k and l); finally, the upper end of the probe is connected with the permeameter (white box on the left) using a vinyl tubing (m). Photos from a to j are taken from the RADON JOK manual (Radon v.o.s).

a specially designed probe (manufactured by Radon v.o.s.) with a constant surface of contact between the probe head and the soil. The constant active area is created in the head of the probe (driven into the soil to about 80 cm depth) by the extrusion of a lost tip by means of the punch wire inside the probe by an exact distance (Fig. 1). The internal volume of the cavity, which is created at the lower end of the sampling probe, is large enough to enable the sample collection. The probes use the approximation $L > d$, with a shape factor $F = 0.149$ m ($L = 50$ mm, $d = 12$ mm and $D = 825$ mm).

The experimental setup consists of a miniature vacuum pump produced by Fürgut GmbH, connected to a vacuum gauge, manufactured by SMC, with a rated pressure range between 0 and -101 kPa. A flux meter from 0 to 5 L min^{-1} (produced by Key Instruments) was originally included in the experimental arrangement. A battery is used to provide energy to instruments (Fig. 2). The pressure gauge is connected via vinyl tubing to the head of the probe on one side and to the pump on the other. Air from the pump was then made to flow through the flux meter and finally escape to the outer environment. The vinyl tubings and metal connectors (components 6 and 7 in Fig. 1) have been kept to a minimum to reduce gas leakage.

Measurements carried out using this equipment were compared with those obtained by RADON JOK (Radon v.o.s, www.radon-vos.cz) which is widely employed in the Czech Republic (Nezmal et al., 2004) and all over the world (Castelluccio et al., 2012; Friske et al., 2010; Xiao et al., 2012) to determine intrinsic permeability of soil. RADON JOK is also quoted in the frame of the European Geogenic Radon Map developed by the Joint Research Centre of the European Commission, as part of its projected European Atlas of Natural Radiation. Soil effective permeability is there considered among controlling variables to quantify the geogenic radon potential (Gruber et al., 2013).

The new permeameter and RADON JOK were connected to the same probe in a variety of geological settings to detect the value of k of different bedrocks (tuffs, travertine, flysch and sands outcropping in Latium region, central Italy), characterized by a large range of permeability. The flow Q and the pressure difference ΔP (sign-changed, vacuum gauge readings) associated with each determination were inserted in Eq. (1) to obtain the gas permeability of soil, either using the new equipment or RADON JOK.

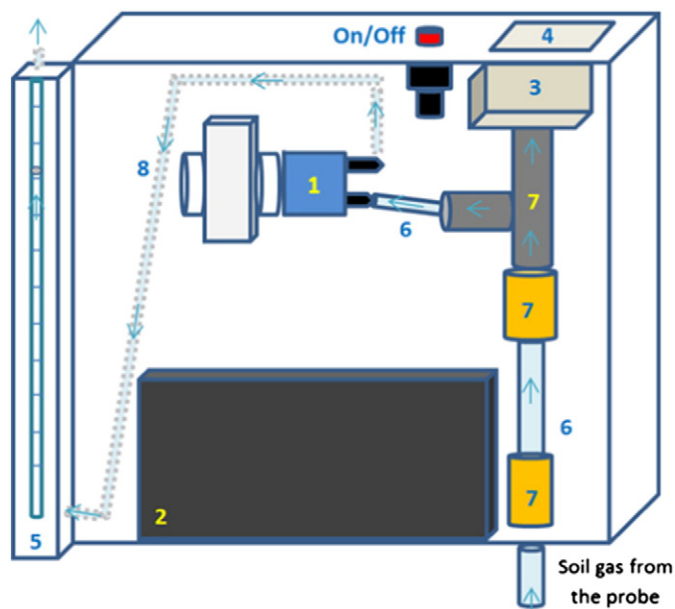


Fig. 2. New permeameter. It consists of a vacuum pump (1), a battery (2), a vacuum gauge (3), with digital display (4) a fluxmeter (5), vinyl tubings (6), metal connectors (7) and electric cables (not shown). Tubings (8) connecting the pump output to the fluxmeter inlet were removed, along with the fluxmeter, at the end of the calibration test (see text for explanation). The arrows indicate air flow within the experimental apparatus.

4. Results and discussion

Table 1 reports the dataset used to create Fig. 3, where air flow data (Q) are plotted against the pressure difference (ΔP), associated with each permeability determination using the new permeameter. Pressure difference data in Table 1 correspond to vacuum gauge readings, because before any measurement the pressure is set to zero and a negative pressure difference compared to the atmospheric value (starting value) is displayed.

Experimental data are aligned along a curve, whose slope $2 \times 10^{-9} \text{ m}^3 \text{ s}^{-1} \text{ Pa}^{-1}$ is here compared with that provided by Fürgut GmbH for the pump operating in free air condition. Field data slope is lower than that given by Fürgut (http://www.fuergut.com/pdfs/dc12_fk.pdf), which is $3 \times 10^{-9} \text{ m}^3 \text{ s}^{-1} \text{ Pa}^{-1}$. Moreover, the value of the intercept on the Y axis is about $6.75 \times 10^{-5} \text{ m}^3 \text{ s}^{-1}$, rather than $7.33 \times 10^{-5} \text{ m}^3 \text{ s}^{-1}$ in free air condition. This demonstrates the reduction of the air flow

Table 1

Air flow (Q), pressure difference (Dp) and gas permeability data determined using the new permeameter ($k1$), compared with RADON-JOK permeability ($k2$). $1.80 \cdot 10^{-11}$ is the upper detection limit of RADON JOK. Dp data correspond to vacuum gauge readings, because before starting the measurement the pressure is set to zero and a negative pressure difference, compared to the atmospheric value (starting value), is displayed.

Identifier	Q ($\text{m}^3 \text{ s}^{-1}$)	DP (Pa)	$k1$ (m^2)	$k2$ (m^2)
1	6.23E-05	-2400	3.05E-12	2.80E-12
2	5.00E-05	-8500	6.91E-13	6.40E-13
3	6.50E-05	-400	1.91E-11	1.40E-11
4	6.50E-05	-800	9.54E-12	7.50E-12
5	6.58E-05	-700	1.10E-11	9.10E-12
6	6.17E-05	-2500	2.90E-12	2.70E-12
7	5.83E-05	-4900	1.40E-12	1.20E-12
8	6.00E-05	-3900	1.81E-12	1.80E-12
9	6.58E-05	-800	9.67E-12	8.00E-12
10	6.25E-05	-1500	4.89E-12	3.40E-12
11	6.50E-05	-700	1.09E-11	>1,80E-11
12	6.67E-05	-500	1.57E-11	>1,80E-11
13	6.67E-05	-300	2.61E-11	1.70E-11
14	6.75E-05	-500	1.59E-11	1.30E-11
15	6.58E-05	-700	1.10E-11	1.70E-11
16	6.57E-05	-700	1.10E-11	>1,80E-11
17	5.17E-05	-8400	7.22E-13	6.30E-13
18	4.58E-05	-11600	4.64E-13	4.50E-13
19	6.42E-05	-1300	5.80E-12	4.90E-12
20	5.58E-05	-6200	1.06E-12	9.00E-13
21	4.83E-05	-9100	6.24E-13	5.10E-13
22	4.67E-05	-10000	5.48E-13	6.10E-13
23	4.17E-05	-12000	4.08E-13	4.00E-13
24	6.58E-05	-900	8.59E-12	5.40E-12
25	6.33E-05	-1800	4.13E-12	4.00E-12
26	6.67E-05	-300	2.61E-11	1.80E-11
27	6.25E-05	-2000	3.67E-12	3.50E-12
28	6.58E-05	-800	9.67E-12	7.10E-12
29	5.00E-05	-8700	6.75E-13	9.20E-13
30	6.50E-05	-1500	5.09E-12	4.00E-12
31	6.58E-05	-1900	4.07E-12	3.70E-12
32	6.67E-05	-700	1.12E-11	8.50E-12
33	6.75E-05	-300	2.64E-11	1.50E-11
34	6.67E-05	-900	8.70E-12	6.10E-12
35	6.67E-05	-500	1.57E-11	1.20E-11
36	6.83E-05	-400	2.01E-11	1.60E-11
37	6.50E-05	-1100	6.94E-12	5.50E-12
38	6.51E-05	-1100	6.95E-12	6.10E-12
39	6.67E-05	-200	3.91E-11	1.20E-11
40	6.83E-05	-100	8.03E-11	>1,80E-11
41	6.67E-05	-100	7.83E-11	1.60E-11
42	6.60E-05	-200	3.88E-11	>1,80E-11
43	6.75E-05	-300	2.64E-11	>1,80E-11
44	6.83E-05	-200	4.01E-11	>1,80E-11
45	6.50E-05	-1100	6.94E-12	5.50E-12
46	6.75E-05	-100	7.93E-11	>1,80E-11
47	5.86E-05	-4400	1.56E-12	1.40E-12
48	5.84E-05	-4800	1.43E-12	2.50E-12

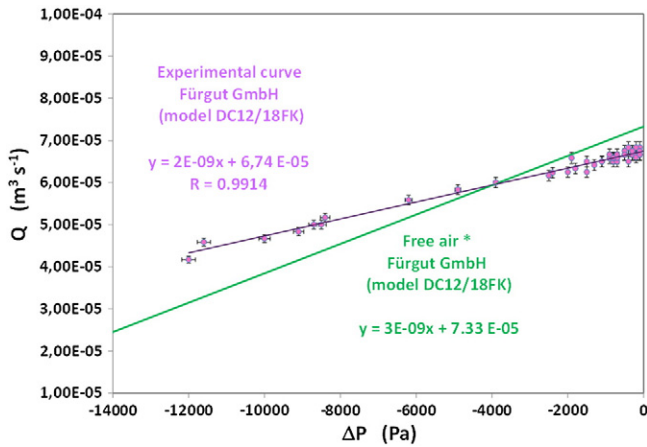


Fig. 3. Experimental air flows (Q) versus pressure gradients (ΔP) measured using the new permeameter, compared to Q - ΔP data provided by Furgüt GmbH for the vacuum pump operating in free air conditions. * Furgüt supplies this diagram (http://www.fuergut.com/pdfs/dc12_fk.pdf) using different units (mbar and L/min) which have been changed here, according to the International System of Units (SI). Errors are given by instrumental sensitivities (fluxmeter and vacuometer).

from the soil through the experimental setup, due to friction/resistance phenomena, reducing the upper limit of air flow and changing the dependence of air flow on pressure difference.

Table 1 reports the whole dataset used to create the experimental graph (Fig. 4) correlating the value of k obtained with the new permeameter (k_1) and that calculated using RADON JOK (k_2). It is worth noting that ten data points are not included in the graph because corresponding k_2 values are higher than the upper limit of RADON JOK equipment (Neznal et al., 2004), which is $1.80 \times 10^{-11} \text{ m}^2$. Fig. 4 shows that variables are very well correlated, demonstrating that the new device provides high quality data, comparable with those obtained with conventional and routinely used instruments.

In addition to that, the new permeameter allows to extend the range of detectable values in the area of high permeability (beyond $1.80 \times 10^{-11} \text{ m}^2$). Moreover, when measuring low permeability data, it provides a quicker response, compared to RADON JOK. For example, the time required to detect a value of k equal to $3.0 \times 10^{-13} \text{ m}^2$ is about 3–4 min using RADON JOK and only few seconds using the new apparatus. With reference to that, it is worth reminding that RADON JOK calculates k value using Eq. (1), where the term Q is not measured directly, but is derived from the ratio between the known air volume which is extracted (2 l) and the time required to complete this action

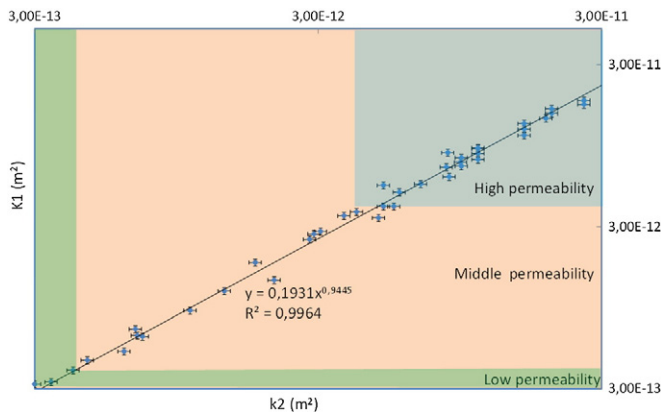


Fig. 4. k_1 (gas permeability using the new permeameter) versus k_2 (gas permeability using RADON JOK) measured from the same probe driven up to 80 cm depth. Permeability classes defined by the Check protocol (Neznal et al., 2004) for assessing the radon risk of building sites are indicated. Errors are given by instrumental sensitivities (fluxmeter and vacuometer for k_1 and chronometer for k_2).

(http://www.radon-vos.cz/?lang=en&lmenu=en_measuring&page=en_measuring_jok). Consequently, the lower the permeability, the longer the time required for extracting the air volume. Moreover, the new instrument is very light (1 kg) and can be easily transported everywhere in the field, even on bumpy and rough terrain.

In conclusion, a further improvement of the experimental assemblage can be envisaged. Since the relationship between the flux and the pressure difference using this equipment is constant (see Fig. 3), it is possible to express the value of Q as a function of ΔP . Introducing this term ($m \Delta P + c$) in Eq. (1), a new calculation may be introduced to determine k only on the basis of ΔP :

$$k = \frac{\mu \cdot (m \Delta P + c)}{F \cdot \Delta P} \quad (3)$$

where m is the slope of the experimental curve (Q vs ΔP) in Fig. 3 and c is the intercept on the Y axis. This allows modifying the experimental device, removing the flux meter (device number 5 in Fig. 2) in order to obtain a simple assemblage consisting of a single pump and a vacuumeter. This new configuration has also the advantage to reduce further the number of connections, minimizing the possibility of gas leakage.

The new device can be employed in the range of 3×10^{-13} – $8.0 \times 10^{-11} \text{ m}^2$, extending the upper detection limit of RADON JOK (1.8×10^{-11}). This is definitely relevant because a higher permeability enables the increased migration of gas through the soil and into the buildings, enhancing the risk. Moreover, it provides rapid responses and is easy to carry in the field.

The new device for in situ measurement of soil permeability may be employed to investigate gases and volatile compounds transport through unsaturated media and to map radon potentials of a given site. With reference to that, the new European Council Directive 2013/59/Euratom of 5 December 2013, identifies soil permeability as a relevant parameter to estimate the distribution of indoor radon concentration to be considered in preparing the national action plans to address long-term risks from radon exposure.

References

Castelluccio, M., Giannella, G., Lucchetti, C., Moroni, M., Tuccimei, P., 2012. La classificazione della pericolosità radon nella pianificazione territoriale finalizzata alla gestione del rischio. Classification of radon hazard in urban planning focused to risk management. *Ital. J. Eng. Geol. Environ.* 2, 5–16.

Damkjær, A., Korsbech, U.A., 1992. A small-diameter probe for in situ measurements of gas permeability of soil. *Radiat. Prot. Dosim.* 45, 85–89.

Fischer, D., Uhrin, C.G., 1996. Laboratory simulation of VOC entry into residence basements from soil gas. *Environ. Sci. Technol.* 30, 2598–2603.

Friske, P.W.B., Ford, K.L., Kettles, I.M., McCurdy, M.W., McNeil, R.J., Harvey, B.A., 2010. North American soil geochemical landscapes project: Canadian field protocols for collecting mineral soils and measuring soil gas radon and natural radioactivity. *Geological Survey of Canada Open File*. 6282, p. 175.

Gan, J., Yates, R.S., Papiernik, S., Crowley, D., 1982. Application of organic amendments to reduce volatile pesticide emissions from Soli. *Environ. Sci. Technol.* 32, 3094–3098.

Gruber, V., Bossew, P., DeCort, M., Tollefsen, T., 2013. The European map of the geogenic radon potential. *J. Radiol. Prot.* 33, 51–60.

Moore, C., Rai, I.S., Lynch, J., 1982. Computer design of landfill methane migration control. *J. Environ. Eng.* 108, 89–107.

Mosley, R.B., Snood, R., Brubaker, S.A., Brown, J., 1996. Experimental evaluation of geometrical shape factor for short cylindrical probes used to measure soil permeability to air. *Environ. Int.* 22, 509–520.

Neznal, M., Neznal, M., Matolin, M., Barnett, I., Miksova, J., 2004. The new method for assessing the radon risk of building sites. *Czech Geological Survey Special Papers*. 16. Czech Geological Survey, Prague, (www.radon-vos.cz/pdf/metodika.pdf).

Rathfelder, K., Lang, J.R., Abriola, L.M., 1995. Soil vapor extraction and bioventing: applications, limitations and future research directions. *U.S. Natl. Rep. Int. Union Geod. Geophys.* 1991–1994. *Rev. Geophys.* 33, 1067–1081.

Thibodeaux, L.J., Springer, C., Riley, L.M., 1982. Models and mechanisms for the vapor phase emission of hazardous chemicals from landfills. *J. Hazard. Mater.* 7, 63–74.

Xiao, L., Wang, N.P., Zhou, Z.G., Hu, X.M., Zeng, L.H., 2012. Mapping of soil radon concentration in Zhongshan, Guangdong Province. *Geoscience* 26, 1300–1305.